Pergamon

Int. J. Solids Structures Vol. 34, No. 21, pp. 2733–2754, 1997

0020-7683/97 $17.00 + .00

PII: S0020-7683(96)00180-1

RECEPTANCE MODEL BASED ON ISOTROPIC DAMPING FUNCTIONS AND ELASTIC DISPLACEMENT MODES

K. DOVSTAM
The Aeronautical Research Institute of Sweden, P.O. Box 11021, S-161 11 Bromma, Sweden

(*Received* 18 *July* 1995; *in revised form* 14 *May* 1996)

Abstract—Starting from a fundamental, continuum mechanical, constitutive material damping description, the augmented Hooke's law (AHL) introduced by Dovstam [Dovstam, K. (1995). Augmented Hooke's law in frequency domain. A three-dimensional, material damping formulation. *International Journal of Solids and Structures* **32**, 2835–2852], a linear three-dimensional damped vibration response model for isotropic material is proposed. The derivations, valid for a restricted but important class of cases, are based on general, continuous, elastic vibration modes, Gurtin [Gurtin, M. E. (1972). The linear theory of elasticity. In *Encyclopedia of Physics*, vol. VIa/2, Mechanics of Solids II (eds Flügge, S. and Truesdell, C.). Springer, Berlin]. Material damping is represented by two complex, frequency dependent, damping functions defined directly by constitutive parameters in the isotropic AHL. Alternatively, for isotropic, viscoelastic solids, the damping functions are derived from two stress relaxation functions. Modal damping functions, which define overall "structural" damping in terms of elastic, modal parameters and the two material damping functions, are introduced in the response model. It is shown that the modal damping functions, indirectly, depend on the geometry and boundary conditions of the piece of material under investigation. Introduced are also new, elastic modal parameters which determine the quantitative contribution to the modal damping functions from the two isotropic, material damping functions. The new modal parameters are easily computed using, slightly modified, standard finite element code, and elastic modes resulting from standard finite element eigenvalue analyses. A close agreement between direct finite element calculations and responses predicted using the proposed modal model is obtained for a studied three-dimensional cantilever test plate. © 1997 Elsevier Science Ltd.

NOMENCLATURE

AHL	augmented Hooke's law
$\mathbf{A}$	system matrix defining the coupling between mode coefficient spectra $c_m(\mathbf{u})$
A_{rm}	complex, s-dependent, matrix element in $\mathbf{A}$
a_m	modal mass corresponding to elastic displacement mode $\mathbf{w}^{(m)}$
C_{ik}	low frequency constant in receptance model for point excited freely moving solid
$c_m(\mathbf{v})$	generalised Fourier coefficient of vector field $\mathbf{v}(\mathbf{x})$ corresponding to mode $\mathbf{w}^{(m)}$
$\mathbf{D}$	spatial, first order, partial differential operator matrix (6×3 operator matrix)
$\mathbf{D}^{\mathrm{T}}$	spatial, first order, partial differential operator; the 3×6 matrix transpose of $\mathbf{D}$
d_G	complex, s-dependent, material damping function of isotropic solid
d_L	complex, s-dependent, material damping function of isotropic solid
$\mathbf{E}$	six-dimensional infinitesimal (engineering) strain vector, $\mathbf{E} = \mathbf{D}[\mathbf{u}]$
$\mathbf{F}$	three-dimensional localised excitation force (point force) on $\partial\Omega$
$F_i^{(m)}$	modal force corresponding to the traction vector field $\mathbf{t}_n$ on $\partial\Omega$
G	elastic shear modulus, Lamé's shear constant (Pa)
$\mathbf{H}$	real, symmetric material modulus 6×6-matrix in Hooke's generalised law (Pa)
$\mathbf{H}_G$	real, diagonal 6×6-matrix in isotropic Hooke's generalised law
$\mathbf{H}_L$	real, symmetric 6×6-matrix in isotropic Hooke's generalised law
$\hat{\mathbf{H}}$	complex, symmetric material modulus 6×6-matrix in augmented Hooke's law
$\mathbf{K}_G$	partial, global stiffness matrix of isotropic, elastic finite element model of $\mathbf{u}$
K_{ik}^N	complex, high frequency correction in receptance model for point excited solid
$\mathbf{L}$	second order, spatial differential operator corresponding to elastic Hooke's law
$\hat{\mathbf{L}}$	second order, spatial differential operator for (solid) AHL material
m, r	mode number indices
l	indexing number for thermodynamic (damping) processes and AHL parameters
N_a	total number of anelastic, thermodynamic (damping) processes
N	number of terms in truncated generalised Fourier series representation of $[\tilde{\mathbf{u}}]$
$\mathbf{n}$	outer unit normal vector on $\partial\Omega$ with Cartesian components $n_k = n_k(\mathbf{x})$
$\mathbf{N}$	Cartesian 3×6-matrix representation of the unit normal $\mathbf{n} = \mathbf{n}(\mathbf{x})$
$\mathbf{R}$	3×3 receptance matrix for force excitation at $\mathbf{x}_e$ and response $\tilde{\mathbf{u}}$ at $\mathbf{x}$
R_{ik}	complex, s-dependent, matrix element in $\mathbf{R}$
s	complex frequency (Laplace variable) with imaginary part ω (frequency in rad/s)

t	time variable
$\mathbf{t}_n$	the traction (stress) vector field on $\partial\Omega$ with Cartesian components $t_k = n_i\sigma_{ik}$
$[\mathbf{t}_n]$	Cartesian 3×1-matrix representation of the traction vector field $[\mathbf{t}_n] = \mathbf{N}\sigma$
$\mathbf{u}$	three-dimensional displacement field with Cartesian components $u_k = u_k(\mathbf{x}, t)$
$[\mathbf{u}]$	Cartesian 3×1-matrix representation of the displacement field $\mathbf{u} = \mathbf{u}(\mathbf{x}, t)$
$\mathbf{U}$	global node displacement vector of finite element model of $\mathbf{u} = \mathbf{u}(\mathbf{x}, t)$
$U_H^{(m)}$	modal strain energy for elastic normal mode $\mathbf{w}^{(m)}$ and elastic material matrix $\mathbf{H}$
$\mathbf{w}^{(m)}$	three-dimensional normal mode with Cartesian components $w_k^{(m)} = w_k^{(m)}(\mathbf{x})$
$[\mathbf{w}^{(m)}]$	Cartesian 3×1-matrix representation of the modal field $\mathbf{w}^{(m)} = \mathbf{w}^{(m)}(\mathbf{x})$
$\mathbf{x}$	point in three-dimensional space with rectangular Cartesian coordinates x_1, x_2, x_3
$[\mathbf{x}]$	Cartesian 3×1-matrix representation of $\mathbf{x}$
$\mathbf{x}_e$	excitation point on $\partial\Omega$, point of action of localised three-dimensional force $\mathbf{F}(t)$
α_I	"dissipation" parameter in isotropic AHL (Pa)
β_I	frequency parameter in AHL, inverse of relaxation time (rad/s)
γ_{rm}	modal coupling factor for damped, isotropic solid
δ_{ik}	Kronecker's delta
ε_{ik}	infinitesimal, Cartesian, strain tensor component corresponding to $\mathbf{u} = \mathbf{u}(\mathbf{x}, t)$
$\varepsilon_{ik}^{(m)}$	infinitesimal, Cartesian, modal strain tensor component corresponding to $\mathbf{w}^{(m)}(\mathbf{x})$
η_G	loss factor, corresponding to the shear modulus G, of isotropic solid
η_λ	loss factor, corresponding to the Lamé modulus λ, of isotropic solid
η_m	modal loss factor corresponding to mode damping function $d_m(s)$
λ	Lamé's constant (Pa)
μ_I	thermodynamic coupling parameter in isotropic AHL (Pa)
μ_{rm}	modal coupling factor for damped, isotropic solid
ν	Poisson's ratio for isotropic, elastic solid
$\bar{\nu}$	complex, frequency dependent Poisson's ratio for isotropic AHL material
ρ	mass density field
$\boldsymbol{\sigma}$	six-dimensional stress vector corresponding to the engineering strain vector $\mathbf{E}$
σ_{ik}	symmetric, Cartesian, stress tensor component (Pa)
φ_I	thermodynamic coupling parameter in isotropic AHL (Pa)
χ_m	modal, damping weight-factor for isotropic solid
$\boldsymbol{\psi}^{(m)}$	mass-normalised modal displacement field corresponding to $\mathbf{w}^{(m)}$
Ψ	specific material damping capacity
ω	circular frequency (rad/s) corresponding to frequency $f = \omega/2\pi$ in Hz
ω_d	damped, circular resonance frequency in rad/s
ω_m	undamped (elastic), circular eigenfrequency in rad/s
Ω	volume in three-dimensional space
$\partial\Omega$	boundary of three-dimensional volume Ω
$\tilde{\mathbf{u}}$	the Laplace transform of $\mathbf{u} = \mathbf{u}(\mathbf{x}, t)$ with respect to the time variable t
$(\mathbf{u}, \mathbf{v})$	inner product of complex, three-dimensional vector fields $\mathbf{u}$ and $\mathbf{v}$ defined in Ω
$(\mathbf{u}, \mathbf{v})_\partial$	inner product of complex, three-dimensional vector fields $\mathbf{u}$ and $\mathbf{v}$ defined in $\partial\Omega$
$\langle \mathbf{A}, \mathbf{B} \rangle$	inner product of complex, six-dimensional vector fields $\mathbf{A}$ and $\mathbf{B}$ defined in Ω.

1. INTRODUCTION

To incorporate models of damping in real life applications, e.g., modelling and prediction of vibroacoustic properties of aircraft, cars, ships and other vehicles, damping parameters have to be estimated for real engineering materials. All new, lightweight and composite engineering materials, constantly increasing in number, therefore must be considered as a great challenge to the vibroacoustic community. Valid for all fundamental constitutive models, including damping models and damping measures, is the fact that material parameters can never be observed directly. As a result there is a growing need for physically representative response models connecting different kinds of damping parameters with experimentally identifiable vibration responses and corresponding excitations.

Starting from the results by Lesieutre (1989–1992), Dovstam (1995) recently developed a linear material damping modelling technique based on internal, thermodynamic variables and formulated as an augmented Hooke's law (AHL) in frequency domain. The damping parameters incorporated in the AHL formulation are material parameters and thus independent of vibration and deformation modes occurring in a particular piece of material. Generally, AHL could handle linear, isothermal but otherwise general damping including high, frequency dependent, non-homogeneous damping. Due to the basic, constitutive formulation of the AHL method, the traditional material damping measures (see, e.g., Bert (1973), Nashif *et al.* (1985), Ewins (1986), Kinra and Wolfenden (1992)) used in the field of sound and vibration can be computed from the AHL parameters once they, and the actual vibrational deformations, are known or given. An inevitable consequence, though, of the basic nature of the AHL parameters, is that currently available experimental modal

analysis (EMA) programs, Ewins (1986), used for estimation of traditional damping parameters, are not suited for estimation of AHL parameters. A reason for this is that available EMA techniques, contrary to the AHL approach, can take into account only constant (frequency independent) proportional, structural and viscous damping resulting in constant modal damping, i.e., a fixed loss factor value for each mode, without link to any material parameters or boundary conditions. New experimental estimation procedures, for AHL material characterisation, are therefore of considerable interest.

With the observations above as background, the objective of the work presented on the following pages was formulated as the definition of an *analytical vibration response model* which could be effectively used in AHL damping parameter estimation based on experimental data from velocity and acceleration frequency response function (FRF) measurements. A displacement response FRF model, meeting these conditions, based on isotropic, uniform AHL and elastic, three-dimensional vibration displacement modes, is presented in Section 4. In this model, damping is represented by the *damping functions* introduced in Section 2.

Although the present paper is based on the AHL formulation, the damping function concept presented could equally be based on traditional *viscoelasticity* (Appendix B) or other available models. Examples of alternative viscoelastic models are *fractional derivative* (Bagley and Torvik, 1983; Enelund and Olsson, 1995) and *mini-oscillator* (Golla and Hughes, 1985; McTavish and Hughes, 1993) *models* of *material modulus functions* (McTavish *et al.*, 1992; McTavish and Hughes, 1993). It is important to note that, independent of the type of damping function model chosen, the presented analytical response model can be used for prediction of vibration responses as well as in damping parameter estimation.

The main contribution of the present paper is: the introduction of isotropic (intrinsic) material damping functions (Section 2); the introduction of modal weights defining the mixed contribution of the two damping functions corresponding to uniform complex, frequency dependent Lamé moduli of isotropic materials (Section 3); the introduction of frequency dependent, modal (structural) damping functions (Section 3), defined entirely by (intrinsic) material parameters and elastic (i.e. undamped) modal parameters; the derivation of explicit expressions for the generalised, modal, Fourier coefficients (Section 3) defining an analytical displacement response model (Section 4) based on uniform, isotropic damping functions and three-dimensional, continuous, elastic, vibration displacement modes.

The modal damping functions introduced here define, analytically, "structural" damping in terms of the "intrinsic" material damping functions for a piece of uniform, isotropic material. They should be compared to the "structural modal damping parameters" discussed by Kinra and Yapura (1992). In fact, the modal loss factors derived here could be used to compute Kinra and Yapura's structural, modal damping parameters in a class of isotropic, three-dimensional cases with uniform damping distribution and completely general geometry and boundary conditions thus linking their modal model with the fundamental AHL relations.

A method, with some similarities to the method proposed here, for prediction of structural damping in terms of material damping loss factors and modal strain energies (MSE), was proposed by Johnson and Kienholz (1982) and modified by Hu *et al.* (1995). These derivations, however, are based on discretised, finite element equations of motion, contrary to the more basic continuum mechanical approach taken here. The variation with frequency of actual storage moduli and corresponding storage stiffnesses, discussed, respectively, by Johnson and Kienholz and Hu *et al.*, is in the present treatment taken into account in the real parts of the material damping functions.

2. GOVERNING EQUATIONS

2.1. *Isotropic augmented Hooke's law*

Throughout the following discussions a three dimensional continuum occupying a volume Ω and obeying the isotropic augmented Hooke's law (Dovstam, 1995), will be considered. Also, Cartesian tensor components and a corresponding matrix notation will

be used. Matrices and vector fields not explained in the main text are explicitly defined in Appendix A where needed for clarity reasons. The summation convention for repeated indices is implied if not otherwise stated or obvious.

The general augmented Hooke's law is formulated in frequency domain as:

$$\tilde{\sigma} = \hat{\mathbf{H}}\tilde{\mathbf{E}} \tag{1}$$

where $\hat{\mathbf{H}} = \hat{\mathbf{H}}(\mathbf{x}, s)$ is a complex, position and a frequency dependent, symmetric, constitutive 6×6 material matrix. For an isotropic AHL material the augmented matrix and corresponding elastic material matrix $\mathbf{H}$ may be expressed, respectively, as 6×6-matrices:

$$\hat{\mathbf{H}} = \mathbf{H} + \lambda \cdot d_\lambda \cdot \mathbf{H}_\lambda + G \cdot d_G \cdot \mathbf{H}_G \tag{2}$$

$$\mathbf{H} = \lambda \cdot \mathbf{H}_\lambda + G \cdot \mathbf{H}_G \tag{3}$$

where λ and G (shear modulus) are the usual elastic Lamé constants (Fung, 1965). The complex, frequency dependent, and generally also position-dependent, *damping functions* d_λ and d_G determine the amount of *material damping* and *dissipation* of mechanical energy in the material and are defined as the functions:

$$d_\lambda(s) = \sum_{l=1}^{N_a} \frac{s}{(s+\beta_l)} \cdot \frac{(3\varphi_l^2 + 4\varphi_l\mu_l)}{\lambda \cdot \alpha_l} \tag{4}$$

$$d_G(s) = \sum_{l=1}^{N_a} \frac{s}{(s+\beta_l)} \cdot \frac{2\mu_l^2}{G \cdot \alpha_l} \tag{5}$$

where the parameters α_l, β_l, φ_l and μ_l, introduced and discussed in Dovstam (1995), are dissipation, relaxation and (two) coupling parameters, respectively, for each of N_a different damping processes in the isotropic AHL. The number of processes, i.e., the number of terms in (4) and (5) needed to describe correctly the stress relaxation, depends on the material and should be considered as a material parameter.

Expressed in terms of the complex moduli $\bar{\lambda}$ and $\bar{G}$ (cf. Appendix B):

$$\bar{\lambda}(s) = \lambda \cdot (1 + d_\lambda(s)) \tag{6}$$

$$\bar{G}(s) = G \cdot (1 + d_G(s)) \tag{7}$$

the constitutive material matrix $\hat{\mathbf{H}}$ is obtained as:

$$\hat{\mathbf{H}} = \bar{\lambda} \cdot \mathbf{H}_\lambda + \bar{G} \cdot \mathbf{H}_G. \tag{8}$$

The corresponding complex, in general frequency dependent, Poisson's ratio $\bar{\nu}(s)$ is:

$$\bar{\nu}(s) = \frac{\bar{\lambda}(s)}{2[\bar{\lambda}(s) + \bar{G}(s)]} = \frac{\nu \cdot (1 + d_\lambda(s))}{\left[1 + \dfrac{\lambda \cdot d_\lambda(s) + G \cdot d_G(s)}{\lambda + G}\right]}. \tag{9}$$

It is obvious then, that the complex Poisson's ratio $\bar{\nu}(s)$ will become real, independent of the frequency s, and equal to the elastic Poisson's ratio ν if the damping functions are identical. Viscoelastic solids and structures with a constant Poisson's ratio has been studied, e.g., by Robertson and Thomas (1971), Robertson (1971) and Yiu (1993).

A case with proportional damping (see, e.g., Ewins (1986) and Hu *et al.* (1995)), may be defined by any, isotropic or anisotropic, elastic Hooke's law matrix $\mathbf{H}(\mathbf{x})$ and an

augmented Hooke's law matrix defined as $\hat{\mathbf{H}} = (1 + d(s))\mathbf{H}(\mathbf{x})$ where $d(s)$ is a complex, analytical function approaching zero for small $|s|$. This corresponds to a damping model with *only one* uniform damping function. It should be noted that *at least two* damping functions, each associated with a modulus in the elastic Hooke's law matrix, are needed in the general isotropic case. In the isotropic case proportional material damping corresponds to a constant, i.e., uniform and frequency independent, complex Poisson's ratio $\bar{\nu}$ in the actual frequency range. Generally, proportional damping can occur in a frequency range *only* if all elastic moduli in $\mathbf{H}$ have corresponding damping functions which are identical in that range.

In the following the *isotropic* case with *uniformly distributed, non-proportional damping*, represented by two complex, frequency dependent damping functions, $d_\lambda = d_\lambda(s)$ and $d_G = d_G(s)$, will be discussed. The elastic properties are assumed to be isotropic and defined by the elastic (generalised) Hooke's law matrix (3).

2.2. *Frequency domain equations of motion*

Assuming zero body forces and zero initial conditions for the displacement field $\mathbf{u} = \mathbf{u}(\mathbf{x}, t)$ and the corresponding velocity field $\dot{\mathbf{u}} = \dot{\mathbf{u}}(\mathbf{x}, t)$, Laplace transformation of the linearized continuum mechanical equations of motion yields the matrix equation:

$$-\mathbf{D}^{\mathrm{T}}[\tilde{\sigma}] + s^2\rho\tilde{\mathbf{u}} = 0 \quad \mathbf{x} \in \Omega \tag{10}$$

for a continuum occupying the volume Ω in three dimensional space.

When stresses, defined according to the isotropic augmented Hooke's law, (1)–(3), are introduced into this equation the resulting frequency domain, partial differential equation for the transformed displacement field $\tilde{\mathbf{u}} = \tilde{\mathbf{u}}(\mathbf{x}, s)$ is obtained as:

$$\hat{\mathbf{L}}[\tilde{\mathbf{u}}] + s^2\rho\tilde{\mathbf{u}} = 0 \quad \mathbf{x} \in \Omega. \tag{11}$$

The frequency dependent, second order, spatial differential operator matrix $\hat{\mathbf{L}}$ is defined as:

$$\hat{\mathbf{L}}[\mathbf{v}] = -\mathbf{D}^{\mathrm{T}}[\hat{\mathbf{H}}\mathbf{D}[\mathbf{v}]] \quad \mathbf{x} \in \Omega \tag{12}$$

for smooth enough three dimensional vector fields $\mathbf{v}$ with complex component fields v_k.

The boundary conditions for the complex, transformed displacement field $\tilde{\mathbf{u}}$ could either be mixed conditions with zero essential conditions for $\tilde{\mathbf{u}}$:

$$\tilde{\mathbf{u}} = 0 \quad \mathbf{x} \in \partial_u\Omega \tag{13}$$

$$\tilde{\mathbf{t}}_n = \hat{\mathbf{t}}(\mathbf{x}, s) \quad \mathbf{x} \in \partial_t\Omega = \partial\Omega - \partial_u\Omega \tag{14}$$

where $\partial\Omega$ is the boundary of Ω. This corresponds to a body fixed in space over the part $\partial_u\Omega$ of the boundary. Alternatively, a freely moving body, excited on the boundary, has the corresponding natural conditions for $\tilde{\mathbf{u}}$ given by (14) with the traction field:

$$[\tilde{\mathbf{t}}_n] = \mathbf{N}\tilde{\sigma} \tag{15}$$

specified by $\hat{\mathbf{t}}(\mathbf{x}, s)$ over the whole boundary $\partial\Omega = \partial_t\Omega$. Here the outward, unit, normal vector field $\mathbf{n}$ is represented by the 3×6 normal vector matrix field $\mathbf{N} = \mathbf{N}(\mathbf{x})$.

3. DISPLACEMENT MODES AND MODE SERIES

3.1. *Introduction*

The elastic free vibration problem and *normal modes* (i.e., real, elastic displacement modes) have been thoroughly investigated by Gurtin (1972). In particular he discusses the

completeness of the normal modes and Parseval's identity for the corresponding (generalised) *Fourier coefficients*. The results are valid for fully three-dimensional, anisotropic, *elastic* bodies.

It seems reasonable to assume that also damped vibrations could be described, essentially, using linear combinations of normal modes when the imaginary parts of the involved damping functions are small compared to unity for the studied frequencies. Whether the damping should be considered small depends on the specific case. However, damping is usually considered as high in an engineering application when the imaginary part of the damping function is of the order of 0.1 (cf. Nashif *et al.* (1985), Snowdon (1968)). Compared to the damping in steel and many fibre composites also a damping function with imaginary part of the order of 0.01 would be considered as high. In cases with small damping, coupling between the modes can be neglected and the damped modes may then be considered as uncoupled, exactly as the elastic, normal modes. High damping cases with *heavily coupled modes* will be only briefly discussed here.

Gurtin's results constitute a suitable starting point for discussion of linear vibrations in general and they are therefore, together with the theory of Hilbert spaces and generalised Fourier series, taken as the mathematical basis for the following discussion of damped vibrations in AHL materials. Inner products $(\mathbf{u}, \mathbf{v})$, $(\mathbf{u}, \mathbf{v})_\partial$ and $\langle \mathbf{A}, \mathbf{B} \rangle$ as well as partial integration formulas used are explicitly defined in Appendix C. The reader is referred to Oden (1979) and Reddy (1986) for mathematical details.

3.2. *Generalised Fourier series based on real modes*

Due to the completeness of the normal modes it is easily shown that a truncated generalised Fourier series for the transformed displacement field $\tilde{\mathbf{u}} = \tilde{\mathbf{u}}(\mathbf{x}, s)$ in a body fixed in space, can generally be expressed as:

$$\tilde{\mathbf{u}}_N(\mathbf{x}, s) = \sum_{m=1}^{N} c_m(\tilde{\mathbf{u}}) \mathbf{w}^{(m)}(\mathbf{x}) \approx \tilde{\mathbf{u}} \quad \mathbf{x} \in \Omega, \quad N < \infty \tag{16}$$

where the $\mathbf{w}^{(m)}$, $m = 1, 2, 3, \ldots$, are elastic, three-dimensional, *displacement modes*. The *mode coefficients* $c_m(\tilde{\mathbf{u}})$, which are modal coordinates given in frequency domain, are defined as:

$$c_m[\tilde{\mathbf{u}}] = ([\tilde{\mathbf{u}}], \rho[\mathbf{w}^{(m)}])/a_m \tag{17}$$

where a_m, $m = 1, 2, 3, \ldots$, are the modal masses:

$$a_m = (\mathbf{w}^{(m)}, \rho[\mathbf{w}^{(m)}]) \neq 0 \quad m = 1, 2, 3, \ldots . \tag{18}$$

In the general case, with arbitrary damping, the modal terms $c_m(\tilde{\mathbf{u}})\mathbf{w}^{(m)}$ are coupled and mode coefficients $c_m(\tilde{\mathbf{u}})$ and $c_n(\tilde{\mathbf{u}})$ with different indices, $m \neq n$, depend on each other in a way which varies with the frequency s (cf. Sections 3.3 and 4). Note that, even though the series (16), in all cases, converges in a mean square sense (see comment at the end of this section) it is not always possible or simple to derive an expression or a system of equations which explicitly define the values of the mode coefficients without actually knowing the entire field $\tilde{\mathbf{u}} = \tilde{\mathbf{u}}(\mathbf{x}, s)$.

The real displacement modes $\mathbf{w}^{(m)} = \mathbf{w}^{(m)}(\mathbf{x})$ satisfy the differential eqn (11) with vanishing damping, i.e.

$$\mathbf{L}[\mathbf{w}^{(m)}] - \omega_m^2 \rho \mathbf{w}^{(m)} = 0 \quad \mathbf{x} \in \Omega \tag{19}$$

$$\mathbf{L}[\mathbf{v}] = -\mathbf{D}^{\mathrm{T}}[\mathbf{H}\mathbf{D}[\mathbf{v}]] \quad \mathbf{x} \in \Omega \tag{20}$$

where ω_m, $m = 1, 2, \ldots$ are *elastic, undamped, circular eigenfrequencies*. The modes are orthogonal in the sense that:

$$(\mathbf{w}^{(m)}, \rho\mathbf{w}^{(r)}) = a_m\delta_{mr} \tag{21}$$

where δ_{mr} is Kronecker's delta. The boundary conditions satisfied by the modes are such that:

$$(\mathbf{NHE}^{(r)}, \mathbf{w}^{(m)})_{\partial} = 0 \tag{22}$$

for all mode number combinations (r, m) and the *conditions* which are *compatible* with the conditions (13), (14) for $\tilde{\mathbf{u}}$ are:

$$\mathbf{w}^{(m)} = 0 \quad \mathbf{x} \in \partial_u\Omega \tag{23}$$

$$\mathbf{t}_n^{(m)} = \mathbf{NHD}[\mathbf{w}^{(m)}] = 0 \quad [\mathbf{x}] \in \partial_t\Omega = \partial\Omega - \partial_u\Omega. \tag{24}$$

As a conclusion of this section, it may be noted that the eqns (16)–(24) are valid also in inhomogeneous, anisotropic cases and that the series (16) converges in the meaning of the $L_2(\Omega)$-norm, $\|\tilde{\mathbf{u}}\| = \sqrt{(\tilde{\mathbf{u}}, \tilde{\mathbf{u}})}$ (Appendix C). Mean square convergence is here used synonymously with $L_2(\Omega)$-convergence.

3.3. *Mode coefficients and modal damping functions*

Explicit expressions for the mode coefficients $c_m(\tilde{\mathbf{u}})$ may, under certain conditions, be derived from the differential equation (11) and boundary conditions (13), (14), (23) and (24) when the damping functions are independent of the space coordinates, i.e., for *uniform damping* distribution. Taking the inner product of (11) and $(\mathbf{w}^{(m)})$ and applying (2), (12) and (17) it follows, after partial integration (Appendix C), that:

$$a_m[s^2 + \omega_m^2]c_m(\tilde{\mathbf{u}}) + d_\lambda \cdot \langle \lambda \mathbf{H}_\lambda \tilde{\mathbf{E}}, \mathbf{E}^{(m)} \rangle + d_G \cdot \langle G\mathbf{H}_G \tilde{\mathbf{E}}, \mathbf{E}^{(m)} \rangle = \tilde{F}_{\partial}^{(m)}(s) \tag{25}$$

where $\mathbf{E}^{(m)} = \mathbf{D}[\mathbf{w}^{(m)}]$ and the *mode force spectrum* $\tilde{F}_{\partial}^{(m)}$ is defined as:

$$\tilde{F}_{\partial}^{(m)}(s) = (\tilde{\mathbf{t}}_n, \mathbf{w}^{(m)})_{\partial} = \int_{\partial_t\Omega} [\tilde{\mathbf{t}}_n]^{\mathrm{T}} [\mathbf{w}^{(m)}] \, \mathrm{d}\, \partial\Omega. \tag{26}$$

When the series representation of $\tilde{\mathbf{u}}$ is substituted into the inner products in the left hand member of (25) an approximation of the *mode coefficients* $c_m\tilde{\mathbf{u}}$ are found as the components of the (truncated) solution vector to the linear, coupled, system of equations:

$$\begin{bmatrix} A_{11} & A_{12} & A_{13} & A_{14} & \cdot & \cdot & \cdot \\ A_{21} & A_{22} & \cdot & \cdot & \cdot & \cdot & \cdot \\ \cdot & \cdot & \cdot & \cdot & \cdot & \cdot & \cdot \\ \cdot & \cdot & \cdot & A_{rm} & \cdot & \cdot & \cdot \\ \cdot & \cdot & \cdot & \cdot & \cdot & \cdot & \cdot \end{bmatrix} \begin{bmatrix} c_1(\tilde{\mathbf{u}}) \\ c_2(\tilde{\mathbf{u}}) \\ \cdot \\ c_m(\tilde{\mathbf{u}}) \\ \cdot \end{bmatrix} = \begin{bmatrix} \tilde{F}_{\partial}^{(1)} \\ \tilde{F}_{\partial}^{(2)} \\ \cdot \\ \tilde{F}_{\partial}^{(r)} \\ \cdot \end{bmatrix} \tag{27}$$

where the symmetric matrix elements A_{rm} are given by:

$$A_{rm} = \begin{cases} a_m[\{1 + \chi_m d_G(s) + (1 - \chi_m) d_\lambda(s)\}\omega_m^2 + s^2], & r = m \\ \gamma_{rm}\{d_G(s) - d_\lambda(s)\}, & r \neq m \end{cases}. \tag{28}$$

It is important to note (cf. (25) and (2)) that the mean square convergence of $\tilde{\mathbf{u}}_N$ does not assure that the modal approximations $\langle (\hat{\mathbf{H}} - \mathbf{H})\mathbf{D}[\tilde{\mathbf{u}}_N], \mathbf{E}^{(m)} \rangle$ converge to the desired values $\langle (\hat{\mathbf{H}} - \mathbf{H})\tilde{\mathbf{E}}, \mathbf{E}^{(m)} \rangle$. When these approximations do not converge, eqn (27) will not be valid and the inner products in (25) have to be handled in some other (convergent) way. However,

it turns out that eqn (27) holds, at least approximately, in a large number of situations which are of great importance and of considerable practical interest. When enforcing some further restrictions on $\tilde{\mathbf{u}}_N$ on the boundary $\partial\Omega$, even the approximations $\langle(\hat{\mathbf{H}}-\mathbf{H})\mathbf{D}[\tilde{\mathbf{u}}_N], \mathbf{E}^{(m)}\rangle$ can be assured to converge. As the number of modes goes to infinity, it can be shown that eqn (27) holds exactly, if the mode series (16) converges in the meaning of the L_2-norm not only in Ω, but also on the boundary $\partial\Omega$. That is, if the norm $\|\tilde{\mathbf{u}}-\tilde{\mathbf{u}}_N\|_\partial = \sqrt{(\tilde{\mathbf{u}}-\tilde{\mathbf{u}}_N, \tilde{\mathbf{u}}-\tilde{\mathbf{u}}_N)_\partial}$ goes to zero when N approaches infinity. In the following treatment the truncated version of (27) with a finite number N of mode coefficients $c_m(\tilde{\mathbf{u}})$, is assumed to hold. The discussion is thus restricted to a class of cases where $\|\tilde{\mathbf{u}}-\tilde{\mathbf{u}}_N\|_\partial$ also converges to zero or can be neglected. Modal methods for dealing with the general case with highly damped and heavily coupled modes will be discussed by the author in a forthcoming paper.

The real and mode dependent *coupling factors* γ_{rm} and *weight factors* χ_m are:

$$\gamma_{rm} = \langle G\mathbf{H}_G\mathbf{E}^{(r)}, \mathbf{E}^{(m)}\rangle = 2\cdot\int_\Omega G\cdot\varepsilon_{ik}^{(r)}\varepsilon_{ik}^{(m)}\,\mathrm{d}\Omega \tag{29}$$

$$\chi_m = \frac{\gamma_{mm}}{a_m\omega_m^2} \quad \text{(no sum on } m\text{)} \tag{30}$$

and it can be shown, using (19)–(22) and partial integration, that:

$$\gamma_{rm}+\mu_{rm} = a_r\omega_r^2\delta_{rm} \tag{31}$$

where the parameters μ_{rm} are defined as the volume integrals:

$$\mu_{rm} = \langle\lambda\mathbf{H}_\lambda\mathbf{E}^{(r)}, \mathbf{E}^{(m)}\rangle = \int_\Omega \lambda\cdot\mathrm{div}(\mathbf{w}^{(r)})\,\mathrm{div}(\mathbf{w}^{(m)})\,\mathrm{d}\Omega. \tag{32}$$

In cases when there is no significant coupling between the modes, which occurs (under the assumptions above) when the off diagonal elements in (γ_{rm}) all are small enough or when the damping functions are identical (cf. the off diagonal terms in (27), (28)) or when the coupling is neglected, eqn (25) is reduced to:

$$c_m\tilde{\mathbf{u}} = \frac{\tilde{F}_\partial^{(m)}(s)}{a_m[\{1+d_m(s)\}\omega_m^2+s^2]} \quad m = 1,2,3,\ldots \tag{33}$$

where the mode damping function $d_m(s)$ is defined as:

$$d_m(s) = \chi_m\cdot d_G(s)+(1-\chi_m)\cdot d_\lambda(s). \tag{34}$$

It is obvious that the weight factors χ_m, and thus also the damping functions $d_m(s)$, depend on the mode number m and the modal strain fields and accordingly also, indirectly, on geometry and boundary conditions. The mode damping function $d_m(s)$ thus must be viewed as a kind of system damping function determined not only by the material properties $d_G(s)$ and $d_\lambda(s)$. Examples of modal damping functions based on hypothetical material damping functions $d_G(s)$ and $d_\lambda(s)$ and computed modal parameters χ_m for a cantilever test plate are given in Section 5.

The modal loss factor $\eta_m(\omega)$ corresponding to the mode dependent damping function $d_m(s)$ is defined as:

$$\eta_m(\omega) = \frac{\mathrm{Im}(d_m(i\omega))}{1+\mathrm{Re}(d_m(i\omega))} \tag{35}$$

which is equivalent to:

$$\eta_m(\omega) = \chi_m \cdot \frac{(1+\mathrm{Re}\{d_G(i\omega)\})}{(1+\mathrm{Re}\{d_m(i\omega)\})} \cdot \eta_G(\omega) + (1-\chi_m) \cdot \frac{(1+\mathrm{Re}\{d_\lambda(i\omega)\})}{(1+\mathrm{Re}\{d_m(i\omega)\})} \cdot \eta_\lambda(\omega). \tag{36}$$

As a special case it follows that the modal damping functions, and the modal loss factors, will be the same for all modes if the damping is proportional, i.e., when the damping functions $d_G(s)$ and $d_\lambda(s)$ are identical (cf. Section 2.1). As expected, it also follows from (28) that the mode terms are uncoupled when the damping is proportional or zero.

The "damped", circular resonance frequency ω_d, corresponding to an undamped frequency ω_m is here defined as the solution $\omega = \omega_d$ to the equation:

$$(1+\mathrm{Re}\{d_m(i\omega)\}) \cdot \omega_m^2 - \omega^2 = 0 \tag{37}$$

or, equivalently:

$$\omega_d = \omega_m \sqrt{1+\mathrm{Re}\{d_m(i\omega_d)\}}. \tag{38}$$

It follows, thus, that the mode coefficient $c_m(\tilde{\mathbf{u}})$ divided by the modal force spectrum $\tilde{F}_{\hat{c}}^{(m)}(s)$ is purely imaginary at the resonance $s = i\omega_d$ and:

$$\left[\frac{c_m(\tilde{\mathbf{u}})}{\tilde{F}_{\hat{c}}^{(m)}(s)}\right]_{s=i\omega_d} = -\frac{i}{a_m \omega_d^2 \cdot \eta_m(\omega_d)}. \tag{39}$$

It is interesting to compare the modal damping functions $d_m(s)$ and loss factors $\eta_m(\omega)$ introduced here with the "fundamental connection between ... material damping and ... the structural modal damping parameter, Ψ_s" established by Kinra and Yapura (1992). This can be done by identifying Ψ_s with $2\pi \cdot \eta_m(\omega_d)$ where ω_d is the damped, circular resonance frequency. Identifying the material loss factors $\eta_G(\omega)$ and $\eta_\lambda(\omega)$ multiplied by 2π with the specific material damping capacities Ψ_G and Ψ_λ, respectively, it follows that Kinra and Yapura's weight parameters W_G and W_λ, for a mode with damped circular frequency ω_d, correspond to the factors:

$$W_G = \chi_m \cdot \frac{(1+\mathrm{Re}\{d_G(i\omega_d)\})}{(1+\mathrm{Re}\{d_m(i\omega_d)\})} \tag{40}$$

$$W_\lambda = (1-\chi_m) \cdot \frac{(1+\mathrm{Re}\{d_\lambda(i\omega_d)\})}{(1+\mathrm{Re}\{d_m(i\omega_d)\})} \tag{41}$$

in front of $\eta_G(\omega)$ and $\eta_\lambda(\omega)$ in (36) evaluated at $\omega = \omega_d$. However, note that Kinra and Yapura (1992), in their article, work with W_E, i.e., the weight parameter corresponding to Young's modulus E, instead of W_λ.

3.4. *Weight factors and modal strain energies*

Following Gurtin (1972) the elastic strain energy U corresponding to the strain (vector) field $\mathbf{E}$ and the elastic, generalised Hooke's material matrix $\mathbf{H}$ is defined as:

$$U = U_H(\mathbf{E}) = \tfrac{1}{2}\langle \mathbf{HE}, \mathbf{E} \rangle \tag{42}$$

for the continuum in a three-dimensional volume Ω. The *modal strain energy* for a *normal mode* $\mathbf{w}^{(m)}$ is correspondingly defined as:

$$U_m = U_H^{(m)} = \tfrac{1}{2}\langle \mathbf{HE}^{(m)}, \mathbf{E}^{(m)} \rangle \tag{43}$$

where $\mathbf{E}^{(m)} = \mathbf{D}[\mathbf{w}^{(m)}]$. Thus, for an *isotropic material*, it follows that:

$$2U_m = \gamma_{mm} + \mu_{mm} = a_m \omega_m^2 \tag{44}$$

which, according to (30), implies that:

$$\chi_m = U_{GH_G}^{(m)} / U_m \tag{45}$$

$$1 - \chi_m = U_{\lambda H_\lambda}^{(m)} / U_m. \tag{46}$$

Hence the weight factor χ_m is *the fraction of the modal strain energy which corresponds to the shear modulus G* while $1 - \chi_m$ is the fraction of the modal strain energy which corresponds to the Lamé modulus λ.

3.5. *Approximate weight and coupling factors*

In practical engineering applications it is usually necessary to resort to finite element (FE) methods for computation of undamped, *elastic eigenfrequencies* and *normal modes*. This is also the case for the *weight* and *coupling factors* discussed above, In fact, it turns out that approximations of the modal coupling factor matrix (γ_{rm}) and weight factors χ_m are easily computed from FE computed, discrete, normal modes $\mathbf{U}^{(m)}$ and a certain partial, global, stiffness matrix. Formally, the computations can be outlined as follows.

According to (29) we have, after an exact partition (see, e.g., Reddy (1986)) into non overlapping elements Ω^e:

$$\gamma_{rm} = \sum_{e=1}^{N_e} \int_{\Omega^e} G \cdot \mathbf{E}^{(r)\mathrm{T}} \mathbf{H}_G \mathbf{E}^{(m)} \, \mathrm{d}\Omega. \tag{47}$$

If the displacement field is *interpolated*, within each element, such that:

$$[\mathbf{u}](\mathbf{x}, t) \approx [\mathbf{u}_e](\mathbf{x}, t) = \mathbf{A}^e(\mathbf{x})\mathbf{U}^e(t) = \mathbf{A}^e(\mathbf{x})\Lambda^e \mathbf{U}(t) \tag{48}$$

then the *approximate strains* $\mathbf{E}^e$ are $\mathbf{E}^e = \mathbf{D}[\mathbf{u}_e] = \mathbf{D}[\mathbf{A}^e]\Lambda^e \mathbf{U} = \mathbf{B}^e \Lambda^e \mathbf{U}$ where $\mathbf{U}$ is the global, discrete displacement vector of the FE model. For the modal strains $\mathbf{E}^{(m)}$ it is obtained that $\mathbf{E}^{(m)} \approx \mathbf{B}^e \Lambda^e \mathbf{U}^{(m)}$ locally, in element Ω^e, and the *approximate expression* for the *modal coupling factor matrix* element γ_{rm} is derived as:

$$\gamma_{rm} \approx \mathbf{U}^{(r)\mathrm{T}} \mathbf{K}_G \mathbf{U}^{(m)}. \tag{49}$$

The global $\mathbf{K}_G$ matrix and the corresponding local element matrices $\mathbf{K}_G^e$ are defined, respectively, as:

$$\mathbf{K}_G = \sum_{e=1}^{N_e} \Lambda^{e\mathrm{T}} \mathbf{K}_G^e \Lambda^e \tag{50}$$

$$\mathbf{K}_G^e = \int_{\Omega^e} G \cdot \mathbf{B}^{e\mathrm{T}} \mathbf{H}_G \mathbf{B}^e \, \mathrm{d}\Omega. \tag{51}$$

Thus, the *partial stiffness matrix* $\mathbf{K}_G$ is defined as the contribution to the total, global elastic stiffness matrix, from the shear modulus part, $G\mathbf{H}_G = \mathbf{H} - \lambda \mathbf{H}_\lambda$, of the elastic Hooke's material matrix $\mathbf{H}$. Facilities for computation of $\mathbf{K}_G$ have recently been implemented in ASKA Acoustics (Göransson, 1988). Note that the FE approximation of the inner product $\langle G\mathbf{H}_G \tilde{\mathbf{E}}, \mathbf{E}^{(m)} \rangle$ in (25) is given by $\tilde{\mathbf{U}}^{\mathrm{T}} \mathbf{K}_G \mathbf{U}^{(m)}$ where $\tilde{\mathbf{U}}$ is the current, global, FE displacement response vector (in s-domain). The corresponding FE approximation of the mode coefficient, implied by the definition (17), is given by $\tilde{\mathbf{U}}^{\mathrm{T}} \mathbf{M} \mathbf{U}^{(m)} / a_m$ and it should agree closely with (33) when the coupling is small. Here $\mathbf{M}$ is the global mass matrix of the FE

model. Thus in applications, the FE approximations above may be used for convergence checks and control of the small coupling assumption.

The weight factors, finally, according to (30) and (49) are approximated as:

$$\chi_m \approx \frac{1}{a_m \omega_m^2} \mathbf{U}^{(m)\mathrm{T}} \mathbf{K}_G \mathbf{U}^{(m)}. \tag{52}$$

It is obvious from (43)–(46) that the χ_m factors are computed with the *same accuracy* as the *square* of the undamped, circular *eigenfrequencies* ω_m when using the approximation (52). Examples of modal parameters χ_m computed with ASKA Acoustics are given in Section 5.

4. DISPLACEMENT RESPONSE DUE TO FORCE EXCITATION

For a body, with arbitrary damping, the displacement field $\tilde{\mathbf{u}}$ can be approximated using the modal expansion (16) once the modal coefficients $c_m(\tilde{\mathbf{u}})$, $m = 1, 2, 3, \ldots, N$ have been computed.

Of special interest, for simulation of vibrational response, is the case when the body is excited by a three-dimensional, dynamic force $\mathbf{F}(t)$ distributed over a small part $\partial_e\Omega$ of the boundary $\partial\Omega$. In this case the modal force spectrum $\tilde{F}_{\partial}^{(m)}$ is given by:

$$\tilde{F}_{\partial}^{(m)} = [\tilde{\mathbf{F}}]^{\mathrm{T}} \mathbf{w}^{(m)}(\mathbf{x}_e) \quad m = 1, 2, 3, \ldots \tag{53}$$

where $\mathbf{x}_e$ is a point on the small area $\partial_e\Omega$ on $\partial_t\Omega = \partial\Omega - \partial_u\Omega$. The *receptances* R_{ik} corresponding to the force spectrum $\tilde{\mathbf{F}}$ at $\mathbf{x}_e$ are defined as the ratios:

$$R_{ik} = R_{ik}(\mathbf{x}, \mathbf{x}_e, s) = \frac{\tilde{u}_i(\mathbf{x}, s)}{\tilde{F}_k(s)} \tag{54}$$

where $\tilde{F}_k(s)$, $k = 1, 2, 3$ are force component spectra.

When the modal coupling, represented by the off diagonal terms in (27), is neglected or zero for all frequencies an explicit, analytical expression for the receptances, here referred to as the (truncated) uncoupled modal receptance model, can be derived as:

$$R_{ik} = \sum_{m=1}^{N} \frac{R_{ik}^{(m)}}{[(1 + d_m(s))\omega_m^2 + s^2]} \tag{55}$$

where the modal parameters $R_{ik}^{(m)}$ and normalised (normal) modes $\boldsymbol{\psi}^{(m)}$ are defined:

$$R_{ik}^{(m)} = \psi_i^{(m)}(\mathbf{x})\psi_k^{(m)}(\mathbf{x}_e) = \psi_i^{(m)}\psi_{ek}^{(m)} \tag{56}$$

$$\boldsymbol{\psi}^{(m)} = \mathbf{w}^{(m)} / \sqrt{a_m}. \tag{57}$$

The contribution from the modes with mode numbers $m > N$ are simple neglected or, as commonly done in experimental modal analysis, accounted for by adding a suitable complex constant $1/K_{ik}^N$ to the truncated mode series (cf. the discussion of residuals in Ewins (1986)). The N dependent complex, constant K_{ik}^N is called the residual stiffness of the truncated receptance.

The receptance model (55) is derived under the assumption that the studied body is constrained, or explicitly stated, fixed in space with zero displacements over the area $\partial_u\Omega$ on the boundary. The derivation in Section 3, alternatively, could be based on free (unconstrained) elastic modes and expressed in a moving coordinate system (accelerating and rotating with the body). It may be shown, though, that the model (55) is valid also in the case of an unconstrained, freely moving body if the Coriolis and centripetal acceleration

effects of the zero frequency, "rigid body", motion is neglected. For a free body a term $C_{ik}/s^2 = 1/(M_{ik}s^2)$ has to be added to the sum in (55), taking care of contributions from the six zero frequency modes (determined by the zero frequency residues), when *retaining* the indices $m = 1, 2, 3, \ldots$ for the elastic (non-rigid), free modes.

Thus, the modal receptance model, with correction for high-frequency modes ($m > N$), may be expressed as:

$$R_{ik} \approx \frac{C_{ik}}{s^2} + \frac{1}{K_{ik}^N} + \sum_{m=1}^{N} \frac{R_{ik}^{(m)}}{[(1+d_m(s))\omega_m^2 + s^2]} \tag{58}$$

where the real, constant parameter C_{ik} is zero if the body is fixed in space. Parameters C_{ik} are easily computed from the mass distribution and geometry of the body together with coordinates of the centre of mass, the response point $\mathbf{x}$ and the excitation point $\mathbf{x}_e$. In applications the undamped, elastic circular frequencies ω_m in (58) may be approximated by results from a finite element eigenvalue analysis. It is interesting then to note that frequency differences $\Delta\omega_m$ due to uncertainties in the elastic moduli G and λ (input data to the eigenvalue analysis), to the first order for given mode shapes, can be predicted as:

$$\frac{\Delta\omega_m}{\omega_m} = \frac{\chi_m}{2} \cdot \frac{\Delta G}{G} + \frac{(1-\chi_m)}{2} \cdot \frac{\Delta\lambda}{\lambda} \tag{59}$$

which follows from eqns (29)–(32) for an isotropic and homogeneous material.

The main difference and fundamental improvement achieved here, compared to results similar to the models (55) and (58) presented in the literature, cf. Ewins (1986), are the modal (structural) damping functions $d_m(s)$. As have been shown, these functions are completely determined by "intrinsic" material damping properties and known elastic undamped, normal mode parameters. It is also evident, from the discussions in Sections 1 and 2, Appendix B and the results in Dovstam (1995), that the intrinsic, material damping function concept is well defined and useful also for anisotropic AHL materials and solid, viscoelastic materials in general. The frequency dependence of the modal damping functions and their link to the frequency dependent material damping functions, representing true material properties, is a fundamental improvement compared to commonly used modal analysis and damping estimation techniques (Ewins, 1986). Extension and generalisation of the modal damping function concept to more complicated, non-homogeneous, built up structures incorporating, e.g., constrained, viscoelastic damping layers (cf. Nashif *et al.*, 1985) is possible and will be discussed by the author in a forthcoming paper.

The validity of the assumption of zero mode coupling (cf. eqns (27) and (28)) is fundamental for the validity of (55) and (58). Therefore, in applications with non-proportional damping not considered as small, the small coupling assumption should be tested by comparing responses from direct FE calculations with responses computed using (58). The damping of the direct FE model and the modal model should then be defined by the same estimated, or otherwise given or predicted, material damping functions d_G and d_λ. Good agreement in such tests assures that the studied case belongs to the class of cases where eqns (27) and (28) are, at least, approximately valid (cf. the convergence discussion in Section 3.3 and the comment on FE approximations in Section 3.5).

5. THREE-DIMENSIONAL TEST EXAMPLE

To test the modal receptance model in Section 4, receptances R_{ik} computed using the modal model have been compared (see below) to corresponding receptances calculated by direct FE response analysis using ASKA Acoustics (Göransson, 1988). When the same AHL parameter values and elastic data are used in both types of response calculations, the results computed with the two methods should agree closely, for a given frequency range, provided that the number of modes, N, and number of elements in the FE model are chosen high enough.

As numerical test object was chosen a cantilever, rectangular plate with the dimensions (standard SI units are used in the following): thickness $h = 0.004$ m, width $b = 0.070$ m and length $L = 0.500$ m. The plate was oriented with the long straight edges parallel to the x-axis ($x = x_1$), with the ends at $x = 0$ and $x = L$, respectively. The displacements $\mathbf{u}$ were constrained to zero in the yz-plane ($y = x_2, z = x_3$) at the fixed end at $x = 0$.

In both the damped, direct response calculations and the undamped, modal parameter calculations (cf. Section 3.5) the plate was modelled using isoparametric, volume elements (20 nodes per element) with one element through the thickness, 14 elements in the y-direction and 100 elements along the x-direction, i.e., a total number of 1400, three-dimensional, almost cubic elements, with three displacement degrees of freedom per node. For this example the new modal parameters, γ_{rm} and χ_m, occurring in the modal model are truly three-dimensional in character.

The elastic material parameters and the mass density, representative for a real polystyrene test piece at room temperature (20°C), was chosen as:

$$G = 0.8824 \cdot 10^9 \text{ Pa}$$

$$\lambda = 2.2689 \cdot 10^9 \text{ Pa}$$

$$\rho = 1050 \text{ kg/m}^3$$

where the G and λ values correspond to the Young's modulus $E_Y = 2.4 \cdot 10^9$ Pa and a Poisson's ratio $\nu = 0.36$.

To simulate isotropic, non-proportional damping in the plate material, hypothetical damping functions d_λ and d_G were defined, by the relations (4) and (5) in Section 2 using three damping processes ($N_a = 3$) and the following AHL damping parameters:

$$\beta_1 = 2\pi \cdot 10, \quad \beta_2 = 2\pi \cdot 100, \quad \beta_3 = 2\pi \cdot 800 \quad \text{[rad/s]}$$

$$\alpha_1 = \alpha_2 = \alpha_3 = 1 \quad \text{[Pa]}$$

$$\varphi_1 = 6000, \quad \varphi_2 = 8000, \quad \varphi_3 = 12{,}000 \quad \text{[Pa]}$$

$$\mu_1 = \mu_2 = \mu_3 = 7500 \quad \text{[Pa]}.$$

The dissipation parameters α_l have been arbitrarily taken to be equal to unity which is equivalent to using normalised thermodynamic coupling parameters $\varphi_l/\sqrt{\alpha_l}$ and $\mu_l/\sqrt{\alpha_l}$ for each damping process. The special choice of three damping processes, with the particular β_l values above, is made in order to generate a high enough damping in the frequency range below 800 Hz. For the chosen numerical test object this frequency regime contains enough resonances (modes) to be suitable for the testing of the modal receptance model.

The real and imaginary parts and loss factor curves, corresponding to the two material damping functions for frequencies in the range 0–800 Hz, are presented in Fig. 1 (Re $[d_G]$, Im $[d_G]$ and η_G) and Fig. 2 (Re $[d_\lambda]$, Im $[d_\lambda]$ and η_λ). Corresponding modal loss factor curves $\eta_m(\omega)$, for five different χ_m factors (modal damping weights) in the range $0.85 \leqslant \chi_m \leqslant 1$, are presented in Fig. 3. The modal loss factor $\eta_m(\omega)$ is identical to the shear modulus loss factor $\eta_G(\omega)$ for modes with $\chi_m = 1$ and $\eta_m > \eta_G$ for modes with $\chi_m < 1$.

The modal coupling factors γ_{rm} and modal damping weights χ_m (cf. Section 3) were calculated for the actual FE plate model, together with the elastic circular eigenfrequencies ω_m and corresponding mode shapes $\mathbf{w}^{(m)}$. Calculated damping weights χ_m for the lowest 100 modes ($\omega_{100}/2\pi = 6642$ Hz and $\omega_{18}/2\pi = 814$ Hz, i.e., 17 modes below 814 Hz) are shown in Fig. 4 and it may be seen that the calculated weights are within the range $0.85 \leqslant \chi_m \leqslant 1$. The modal loss factor curves in Fig. 3 are typical for the modes in the studied cantilever plate. All calculated, normalised coupling factors $\gamma_{rm}/\omega_r\omega_m\sqrt{a_r a_m}$ were smaller than 0.06 for all (r, m) with $r \neq m$ and $r,m \leqslant 100$ and most of them much smaller. Thus, the off-diagonal terms in the normalised coupling factor matrix are small compared to the damping weights (cf. (29) and (30)).

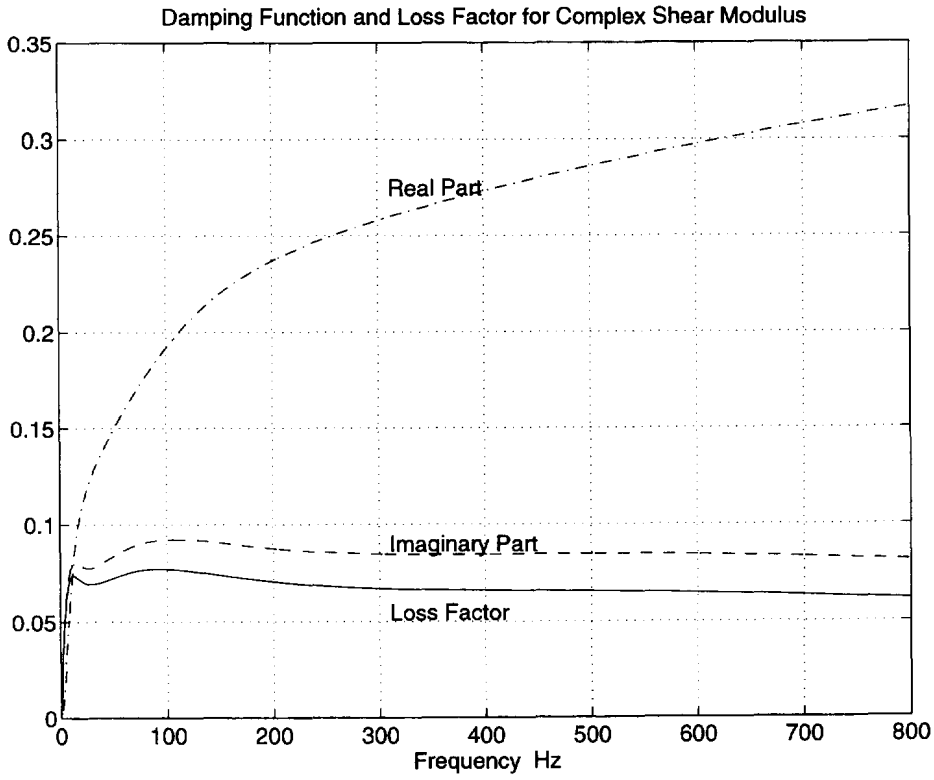

Fig. 1. Damping function d_G (real part, - - - -; imaginary part, - - -) and loss factor η_G (solid line) for complex shear modulus $\bar{G}$ used for cantilever test plate.

Results from modal and direct FE response calculations are presented in Figs 5 and 6. The presented responses are magnitude, displacement spectra $|R_{33}|$ (cf. the definition of R_{ik} in Section 4) for the response point $x = L$, $y = 0$, $z = h$ due to a dynamic force in the z-direction with unit spectrum ($\tilde{F}_z = 1$) at the excitation point $x_e = L$, $y_e = b$, $z_e = h$. The agreement between the results for the uncoupled modal model and direct FE calculations is excellent which can be seen in detail in Fig. 6 (FE solid line, modal dashed line) for the frequency range 200–700 Hz. In Fig. 6 the curves are indistinguishable. The same good agreement between modal and direct FE calculations was obtained in all response directions (only the 3-direction shown here) and for all types of spectra, i.e., magnitude, real part and imaginary part (only magnitude spectra shown here).

Modal and direct FE response calculations, of the same type as above, for two modified cases are presented in Figs 7 and 8. The frequency range 200–700 Hz is the same as in Fig. 6 for the original case. In the case presented in Fig. 7 the same material parameters were used as in the original case (Figs 5–6), except for the μ parameters which were chosen two times the original ones, i.e., $\mu_1 = \mu_2 = \mu_3 = 15{,}000$ Pa. These new parameters result in a damping function d_G which is a factor 4 times the original one and a damping function d_λ which is a factor about 1.5 times the original one. In Fig. 8 the same material parameters were used as in the original case, except for the φ parameters which were chosen to be two times the original ones, i.e., $\varphi_1 = 12{,}000$, $\varphi_2 = 16{,}000$ and $\varphi_3 = 24{,}000$ Pa. The damping function d_G is then the same as the original one and the damping function d_λ is about a factor 2.9 times the original one. Apparently the agreement is extremely good also in the high d_G case (Fig. 7) while it is not quite as good in the high d_λ case (Fig. 8).

The damped resonance frequencies (corresponding to peaks in the receptance curves) are very closely predicted (cf. eqn (38)) in all the studied cases. No significant difference could be observed between modal responses computed using eqn (33) and eqns (27), (28) respectively. The number of modal terms in the modal calculations, coupled as well as uncoupled, was $N = 100$. The frequency step used was $\Delta f = 1$ Hz.

It is concluded that the uncoupled model (dashed line in Figs 6–8) can be used for simulation of the given cantilever test plate for small damping and high damping with AHL

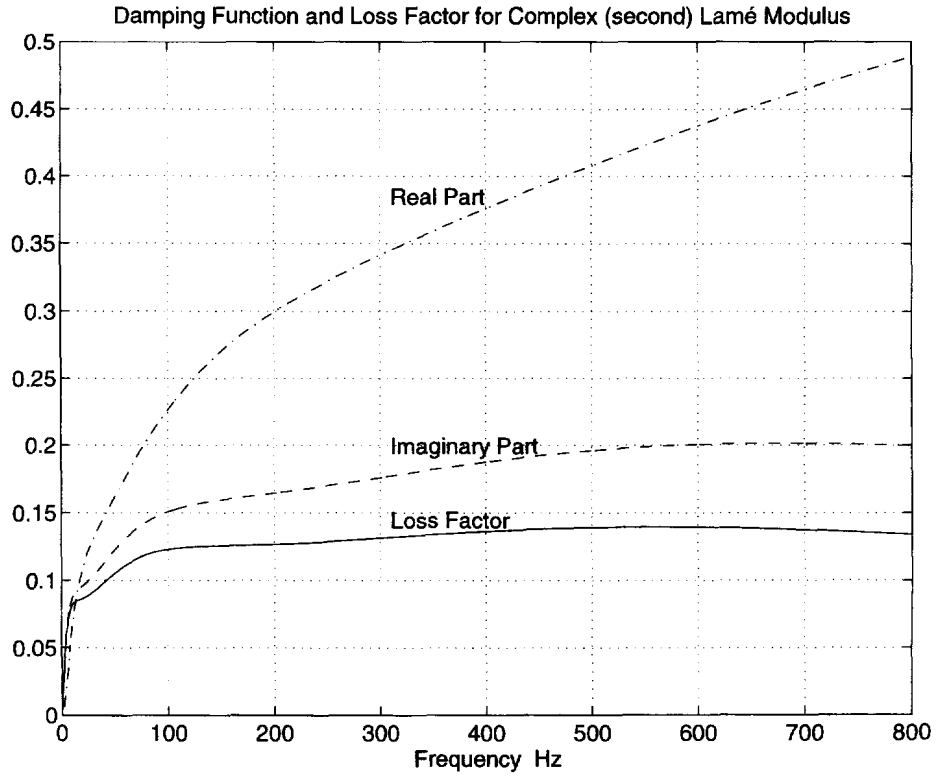

Fig. 2. Damping function d_λ (real part, - · - · ; imaginary part, - - -) and loss factor η_λ (solid line) for complex Lamé $\bar{\lambda}$ used for cantilever test plate.

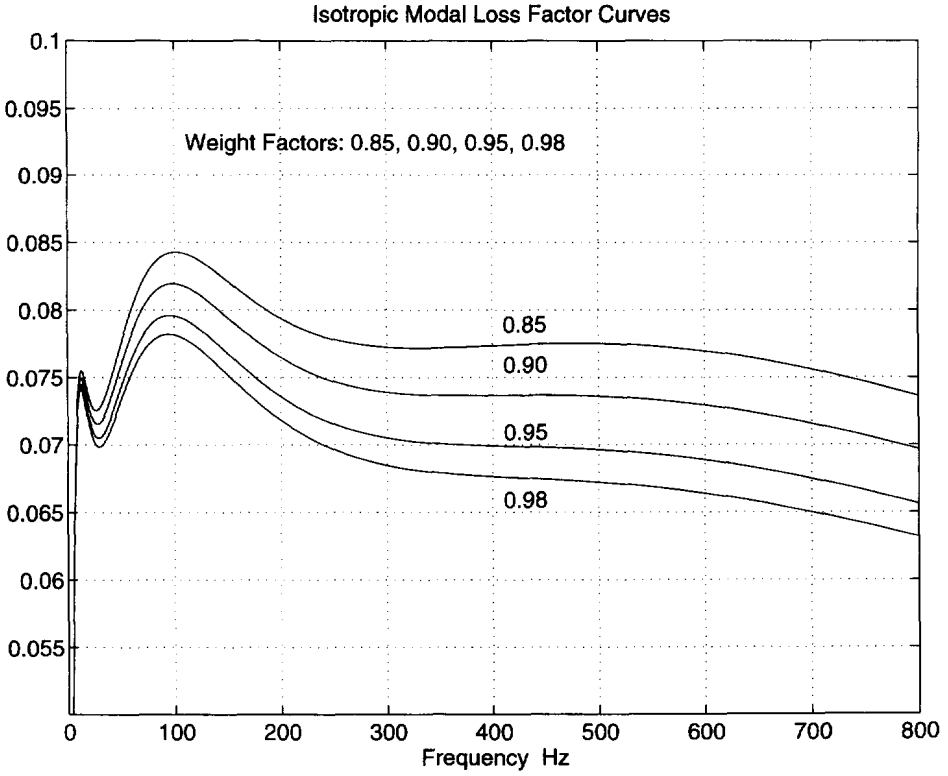

Fig. 3. Isotropic model loss factors $\eta_m(\omega)$ corresponding to d_G and d_λ in Figs 1–2 and modal damping weights χ_m in the range $0.85 \leqslant \chi_m \leqslant 1$.

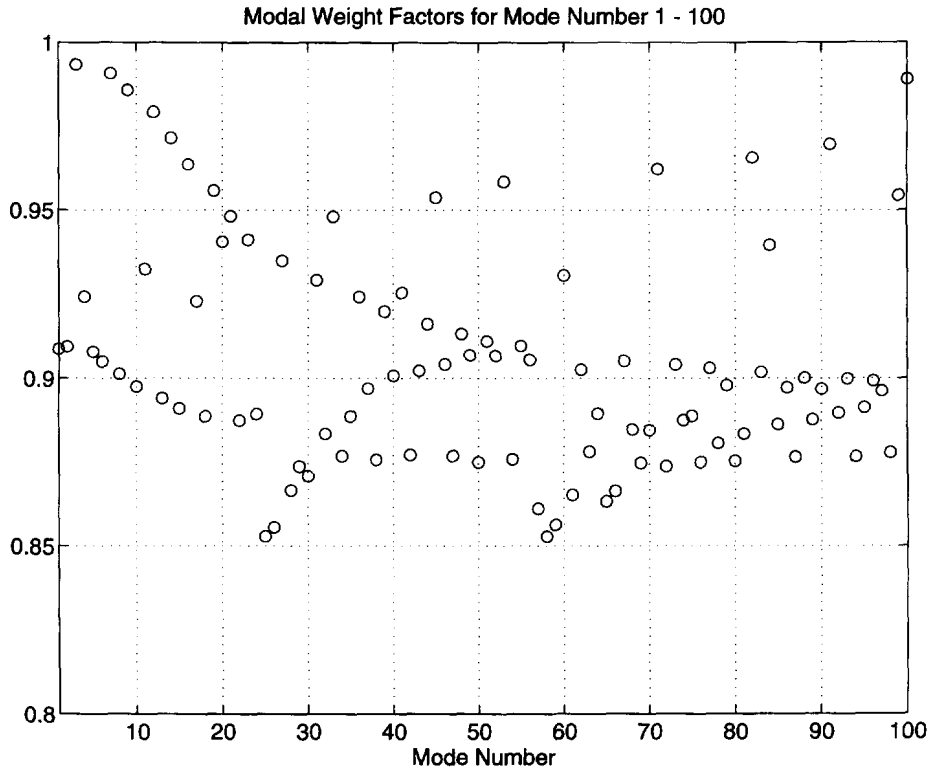

Fig. 4. Calculated modal damping weights χ_m for mode numbers 1–100 of the cantilever test plate.

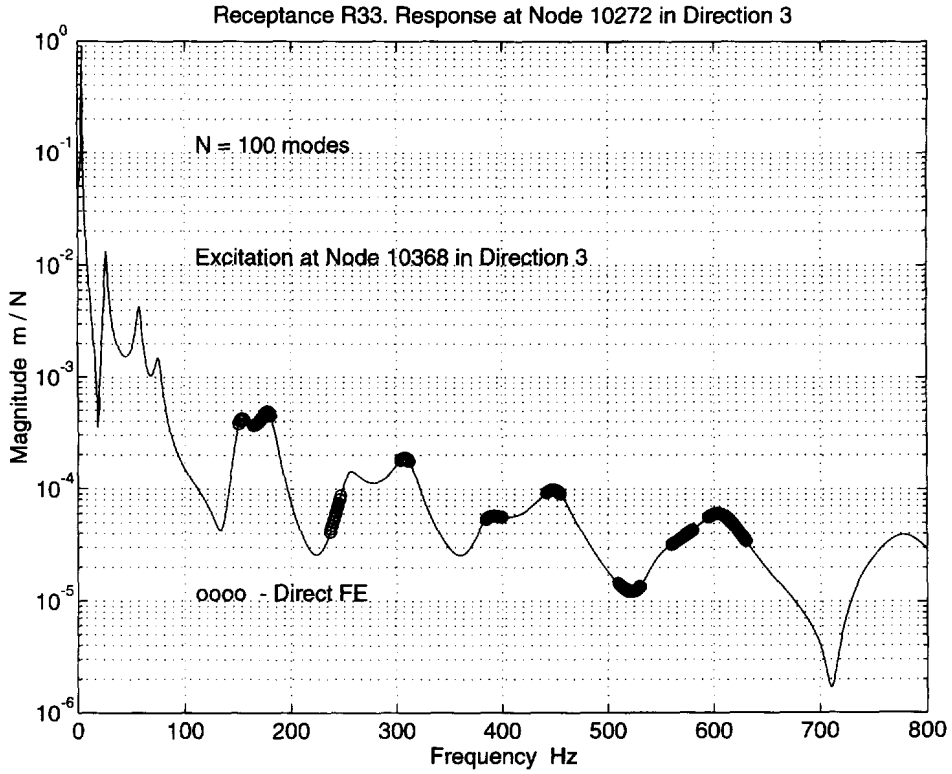

Fig. 5. Absolute value of calculated receptance R_{33}. Response in z-direction in upper corner at free end due to force excitation in the opposite upper corner at the free end. Solid line, uncoupled modal model (eqn (55)) with 100 modes. Circles, direct FE response. Frequency range 0–800 Hz.

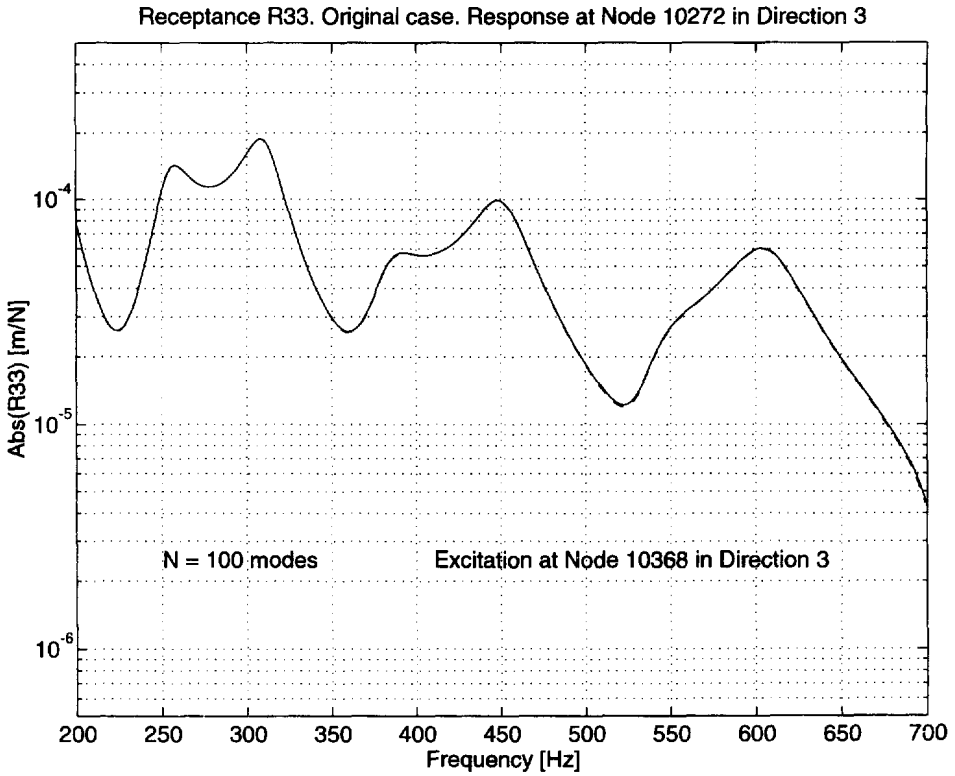

Fig. 6. Absolute value of calculated receptance R_{33}. Response in z-direction in upper corner at free end due to force excitation in the opposite upper corner at the free end. Solid line, direct FE response. Dashed line, uncoupled modal model (eqn (55)) with 100 modes for the same case. Frequency range 200–700 Hz.

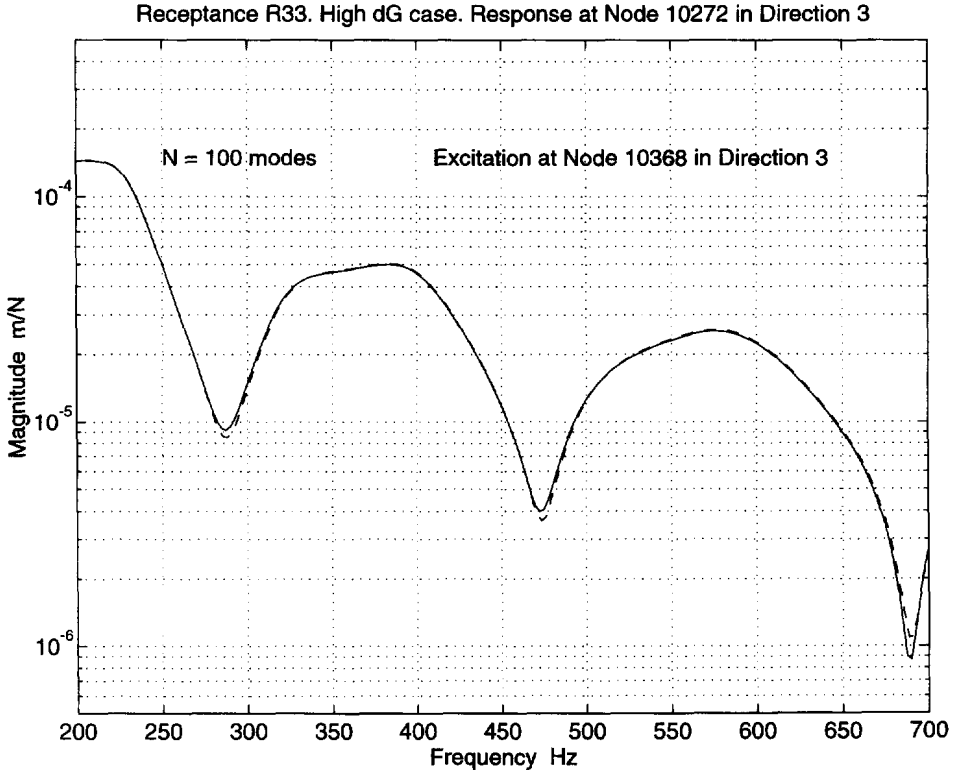

Fig. 7. Absolute value of calculated receptance R_{33}. Response in z-direction in upper corner at free end due to force excitation in the opposite upper corner at the free end. Solid line, direct FE response for the high d_G case. Dashed line, uncoupled modal model (eqn (55)) with 100 modes for the same high d_G case. Frequency range 200–700 Hz.

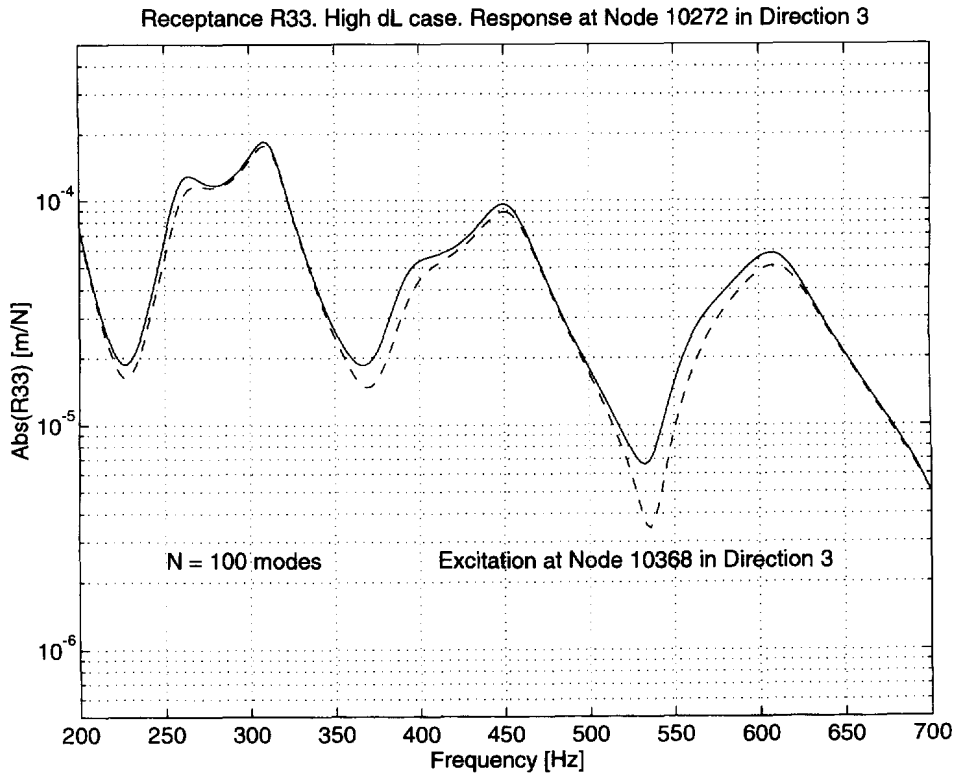

Fig. 8. Absolute value of calculated receptance R_{33}. Response in z-direction in upper corner at free end due to force excitation in the opposite upper corner at the free end. Solid line, direct FE response for the high d_λ case. Dashed line, uncoupled modal model (eqn (55)) with 100 modes for the same high d_λ case. Frequency range 200–700 Hz.

damping parameter combinations $\varphi_l/\sqrt{\alpha_l}, \mu_l/\sqrt{\alpha_l}$ corresponding to the range of values discussed in the examples above. It can also, of course, be used for arbitrarily high proportional damping.

As a conclusion of the discussion an example where the approximations $\langle(\hat{\mathbf{H}}-\mathbf{H})\mathbf{D}[\tilde{\mathbf{u}}_N], \mathbf{E}^{(m)}\rangle$ in (25) are not good and therefore the eqns (27), (28) or (33) are not valid, is shown in Fig. 9. Here the same excitation and material parameters were used as in the original case (Figs 5–6), except for the μ parameters which were chosen 0.1 times the original ones (resulting in d_G a factor 100 times smaller), i.e., $\mu_1 = \mu_2 = \mu_3 = 750$ Pa, and the φ parameters which were chosen as $\sqrt{10}$ times the original ones, i.e., $\varphi_1 = 18{,}974$, $\varphi_2 = 25{,}298$ and $\varphi_3 = 37{,}947$ Pa. The frequency step used in this case was $\Delta f = 2.5$ Hz. The response (solid line) computed using $N = 100$ modes and eqn (16) agrees completely with the direct FE computed response while the modal responses computed using eqns (27), (28) (dotted line) and (33) (dashed line) deviate largely from the correct values. In the fully coupled modal computation the first 100 modal coefficients $c_m(\tilde{\mathbf{u}})$ in (16) was approximated by $\tilde{\mathbf{U}}^{\mathrm{T}}\mathbf{M}\,\mathbf{U}^{(m)}/a_m$ as proposed in Section 3.5. Note that the damping, in terms of modal loss factors and widths of the resonance peaks, is not particularly high in this hypothetical, coupled case.

6. SUMMARY

A linear, three-dimensional damped vibration response model, based on two isotropic, damping functions and three-dimensional, continuous, elastic vibration modes is proposed. The derivations are based on Hilbert space theory and generalised Fourier series.

Material damping is specified through the introduction of two complex, frequency dependent, damping functions defined directly by constitutive, material parameters in the isotropic, augmented Hooke's law (AHL) or, alternatively, by stress relaxation functions for an isotropic, viscoelastic solid.

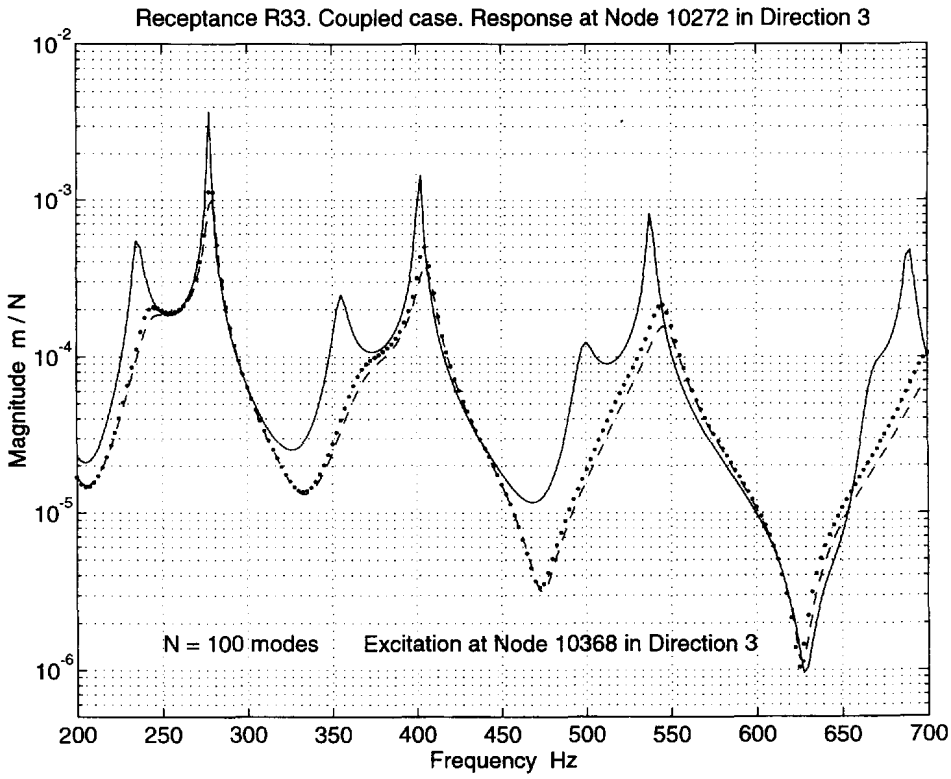

Fig. 9. Absolute value of calculated receptance R_{33}. Response in z-direction in upper corner at free end due to force excitation in the opposite upper corner at the free end. Solid line, modal response computed using eqn (16) and direct FE for the case with very high d_i and very low d_G. Dotted line modal response according to eqns (27) and (28) for the same case. Dashed line, uncoupled modal model response according to eqn (55) for the same case. All modal calculations with 100 elastic, displacement modes. Frequency range 200–700 Hz.

Modal damping functions, which define "structural" damping, for finite pieces of material, in terms of elastic, modal parameters and the two (intrinsic) material damping functions, are introduced. It is shown that the modal damping functions, indirectly, depend on the geometry and boundary conditions of the piece (i.e. a finite volume with boundary) of material under investigation when the material damping functions are different. When the material damping functions are identical, the damping becomes proportional and the modal damping functions all equals the same (frequency dependent) single material damping function.

New, elastic modal parameters are introduced. These determine the quantitative contribution to the modal damping from the two isotropic, material damping functions. The new modal parameters are shown to be easily computed using a slightly modified, standard finite element code, and results from standard finite element eigenvalue analysis.

A close agreement between direct finite element calculations and responses predicted using the proposed modal model is demonstrated for a three-dimensional test case.

For highly (non-proportionally) damped cases the convergence of the uncoupled modal model has to be checked from case to case. Such checks can be carried out using direct FE calculations as outlined in the paper.

Acknowledgements—This work was performed under contract from the Swedish Defence Material Administration (Contract No. 23250-93-102-24-001). The funding provided is gratefully acknowledged.

Many thanks to Peter Göransson (FFA Acoustics department) and Adam Zdunek (FFA Strength of material department) for valuable discussions and criticism. The author is also deeply indebted to Mats Dalenbring (FFA Acoustics department) for doing the necessary ASKA Acoustics (finite element) and MATLAB® (m-files) implementations and actual computations of the new modal parameters and displacement responses for the numerical test case. The author gratefully acknowledge Saab Scania AB for the possibility to implement new facilities in their ASKA finite element code at FFA.

REFERENCES

Bagley, R. L. and Torvik, P. J. (1983) Fractional calculus—a different approach to the analysis of viscoelastically damped structures. *AIAA Journal* **21,** 741–748.

Bert, C. W. (1973) Material damping: an introductory review of mathematical models, measures, and experimental techniques. *Journal of Sound and Vibration* **29,** 129–153.

Dovstam, K. (1995) Augmented Hooke's law in frequency domain. A three-dimensional, material damping formulation. *International Journal of Solids and Structures* **32,** 2835–2852.

Enelund, M. and Olsson, P. (1995) Damping described by fading memory models. *AIAA Paper* #95-1181, 36th Structures, Structural Dynamics and Materials Conference, New Orleans, LA, x–y, April 1995.

Ewins, D. J. (1986) *Modal Testing: Theory and Practice*, Research Studies Press Ltd. and Brüel & Kjaer.

Fung, Y. C. (1965) *Foundation of Solid Mechanics*, Prentice-Hall, London.

Golla, D. F. and Hughes, P. C. (1985) Dynamics of viscoelastic structures—A time domain, finite element formulation. *Journal of Applied Mechanics* **52,** 897–906.

Gurtin, M. E. (1972) The linear theory of elasticity. In *Encyclopedia of Physics*, vol. VIa/2, Mechanics of Solids II (eds Flügge, S. and Truesdell, C.), Springer, Berlin.

Göransson, P. (1988) *ASKA Acoustics. Theory and applications*, FFA TN 1988–13, the Aeronautical Research Institute of Sweden, Stockholm.

Hu, B.-G., Dokainish, M. A. and Mansour, W. M. (1995) A modified MSE method for viscoelastic systems: a weighted stiffness matrix approach. *Journal of Vibration and Acoustics* **117,** 226–231.

Johnson, C. D. and Kienholz, D. A. (1982) Finite element prediction of damping in structures with constrained viscoelastic layers. *AIAA Journal* **20,** 1284–1290.

Kinra, V. K. and Wolfenden, A. (1992) (eds). *M^3D: Mechanics and mechanisms of material damping*, ASTM STP 1169, Americal Society for Testing and Materials, Philadelphia.

Kinra, V. K. and Yapura, C. L. (1992) A fundamental connection between intrinsic material damping and structural damping. *M^3D: Mechanics and mechanisms of material damping*, ASTM STP 1169 (eds V. K. Kinra and A. Wolfenden), American Society for Testing and Materials, Philadelphia, pp. 396–420.

Lesieutre, G. A. (1989) Finite element modelling of frequency-dependent material damping using augmenting thermodynamic fields. Ph.D. dissertation, Aerospace Engineering, University of California, Los Angeles.

Lesieutre, G. A. and Mingori, D. L. (1990) Finite element modelling of frequency-dependent material damping using augmenting thermodynamic fields. *Journal of Guidance Control, Dynamics* **13,** 1040–1050.

Lesieutre, G. A. (1992) Finite elements for dynamic modeling of uniaxial rods with frequency-dependent material properties. *International Journal of Solids and Structures* **29,** 1567–1579.

Lesieutre, G. A. (1992) Finite elements for modeling frequency dependent material damping using internal state variables. *American Society for Testing and Materials, ASTM STP* 1169, pp. 344–357.

McTavish, D. J., Hughes, P. C., Soucy, Y. and Graham, W. B. (1992) Prediction and measurement of modal damping factors for viscoelastic space structures. *AIAA Journal* **30,** 1392–1399.

McTavish, D. J. and Hughes, P. C. (1993) Modeling of linear viscoelastic space structures. *Journal of Vibration and Acoustics* **115,** 103–110.

Nashif, A. D., Jones, D. I. G. and Henderson, J. P. (1985) *Vibration Damping*, John Wiley & Sons, New York.

Oden, J. T. (1979) *Applied Functional Analysis*, Prentice-Hall, Englewood Cliffs, New Jersey.

Reddy, J. N. (1986) *Applied Functional Analysis and Variational Methods in Engineering*, McGraw-Hill, New York.

Robertson, S. R. and Thomas, C. R. (1971) On the forced motion of a viscoelastic solid. *Journal of the Acoustical Society of America* **49,** 1673–1675.

Robertson, S. R. (1971) Using measured material parameters in solving forced motion problems in viscoelasticity. *Journal of Sound and Vibration* **19,** 95–109.

Snowdon, J. C. (1968) *Vibration and Shock in Damped Mechanical Systems*, John Wiley & Sons, New York.

Yiu, Y. C. (1993). Finite element analysis of structures with classical viscoelastic materials. In *Proc. 34th AIAA/ASME/ASCE/AHS/ASC Structures, Structural Dynamics and Materials Conf.* La Jolla, CA, pp. 2110–2119.

APPENDIX A: DEFINITIONS

The Cartesian matrix representations $[\mathbf{u}]$, $\boldsymbol{\sigma}$ and $\mathbf{E}$ of the displacement field and the symmetric stress and (infinitesimal) strain tensor fields respectively are defined as:

$$[\mathbf{u}] = [\mathbf{u}](\mathbf{x}, t) = [u_1 \quad u_2 \quad u_3]^{\mathrm{T}} \tag{A1}$$

$$\boldsymbol{\sigma} = \boldsymbol{\sigma}(\mathbf{x}, t) = [\sigma_{11} \quad \sigma_{22} \quad \sigma_{33} \quad \sigma_{12} \quad \sigma_{23} \quad \sigma_{31}]^{\mathrm{T}} \tag{A2}$$

$$\mathbf{E} = \mathbf{E}(\mathbf{x}, t) = [\varepsilon_{11} \quad \varepsilon_{22} \quad \varepsilon_{33} \quad 2\varepsilon_{12} \quad 2\varepsilon_{23} \quad 2\varepsilon_{31}]^{\mathrm{T}} \tag{A3}$$

where u_i, σ_{ik} and ε_{ik} are Cartesian vector and tensor components. Likewise the matrix representation of the modal displacement field for mode number m is defined as:

$$[\mathbf{w}^{(m)}] = [\mathbf{w}^{(m)}](\mathbf{x}) = [w_1^{(m)} \quad w_2^{(m)} \quad w_3^{(m)}]^{\mathrm{T}}. \tag{A4}$$

The strain vector $\mathbf{E}$, corresponding to the infinitesimal engineering strains, may be determined from the matrix field $[\mathbf{u}]$ as:

$$\mathbf{E} = \mathbf{D}[\mathbf{u}] \tag{A5}$$

where the first order, partial differential operator matrix $\mathbf{D}$ is the Cartesian 6×3-matrix representation:

$$\mathbf{D} = \mathbf{D}[\ ] = \begin{bmatrix} \frac{\partial}{\partial x_1} & 0 & 0 & \frac{\partial}{\partial x_2} & 0 & \frac{\partial}{\partial x_3} \\ 0 & \frac{\partial}{\partial x_2} & 0 & \frac{\partial}{\partial x_1} & \frac{\partial}{\partial x_3} & 0 \\ 0 & 0 & \frac{\partial}{\partial x_3} & 0 & \frac{\partial}{\partial x_2} & \frac{\partial}{\partial x_1} \end{bmatrix}^{\mathrm{T}} \tag{A6}$$

of the three-dimensional, spatial, symmetric gradient operator (Gurtin, 1972). The Cartesian matrix representation $\mathbf{N} = \mathbf{N}\mathbf{x}$ of the unit normal vector $\mathbf{n}$ is defined:

$$\mathbf{N} = \begin{bmatrix} n_1 & 0 & 0 & n_2 & 0 & n_3 \\ 0 & n_2 & 0 & n_1 & n_3 & 0 \\ 0 & 0 & n_3 & 0 & n_2 & n_1 \end{bmatrix}. \tag{A7}$$

The only non-zero elements of the real matrices $\mathbf{H}_\lambda$ and $\mathbf{H}_G$ are:

$$(\mathbf{H}_\lambda)_{ik} = 1 \quad i,k \leqslant 3 \tag{A8}$$

$$(\mathbf{H}_G)_{ii} = 2, \quad 1 \leqslant i \leqslant 3; \quad (\mathbf{H}_G)_{ii} = 1, \quad 4 \leqslant i \leqslant 6. \tag{A9}$$

APPENDIX B: DAMPING FUNCTIONS FOR VISCOELASTIC SOLID MATERIALS

Damping functions d_λ and d_G for isotropic, viscoelastic solids could be defined by requiring, for all s, that:

$$d_\lambda(s) = \bar{\lambda}(s)/\bar{\lambda}(0) - 1 \tag{B1}$$

$$d_G(s) = \bar{G}(s)/\bar{G}(0) - 1 \tag{B2}$$

where $\bar{\lambda}(s)$ and $\bar{G}(s)$ are viscoelastic, frequency dependent, complex moduli (cf., e.g., Snowdon (1968), Nashif *et al.* (1985)) with $\bar{\lambda}(0)$ and $\bar{G}(0)$, respectively, equal to the fully relaxed (long term) elastic Lamé's moduli λ and G.

Generally, if $R(t)$ is one of several stress relaxation functions of a viscoelastic solid the corresponding damping function $d_M(s)$ is defined as:

$$d_M(s) = s \cdot \tilde{R}(s)/M - 1 \tag{B3}$$

where $M = R(\infty) = \lim_{s \to 0} s \cdot \tilde{R}(s)$ is the fully relaxed value of the stress relaxation function, i.e. the relaxed elastic (Hooke's) modulus corresponding to $R(t)$.

APPENDIX C: INNER PRODUCTS

The $L_2(\Omega)$ inner product $(\mathbf{u}, \mathbf{v})$ is defined, (Oden, 1979):

$$\mathbf{u}, \mathbf{v} = \int_\Omega [\mathbf{u}]^{\mathrm{T}} [\mathbf{v}^*] \, \mathrm{d}\Omega \tag{C1}$$

where $\mathbf{v}^*$ denotes the complex conjugate of the three-dimensional vector field $\mathbf{v}$. The natural norm in $L_2(\Omega)$, induced by the inner product $(\mathbf{u}, \mathbf{v})$ is defined as:

$$\|\tilde{\mathbf{u}}\| = \sqrt{(\tilde{\mathbf{u}}, \tilde{\mathbf{u}})} \tag{C2}$$

for the complex vector field $\tilde{\mathbf{u}}$. The inner product $(\mathbf{u}, \mathbf{v})_{\partial}$ for vector fields on the boundary $\partial\Omega$ is defined:

$$(\mathbf{u}, \mathbf{v})_{\partial} = \int_{\partial\Omega} [\mathbf{u}]^{\mathrm{T}} [\mathbf{v}^*] \, \mathrm{d}\partial\Omega \tag{C3}$$

and the $L^2(\Omega)$ inner product $\langle \mathbf{A}, \mathbf{B} \rangle$ of two six-dimensional vector fields is defined:

$$\langle \mathbf{A}, \mathbf{B} \rangle = \int_\Omega \mathbf{A}^{\mathrm{T}} \mathbf{B}^* \, \mathrm{d}\Omega. \tag{C4}$$

Here $\mathbf{B}^*$ denotes the complex conjugate of the six-dimensional vector field $\mathbf{B}$.

For arbitrary three and six dimensional fields $\mathbf{v}$ and $\mathbf{A}$ it may be shown by partial integration [Gauss' theorem] that:

$$(\mathbf{D}^{\mathrm{T}}[\mathbf{A}], \mathbf{v}) + \langle \mathbf{A}, \mathbf{D}[\mathbf{v}] \rangle = (\mathbf{NA}, \mathbf{v})_{\Gamma} \tag{C5}$$

$$\langle \mathbf{D}[\mathbf{v}], \mathbf{A} \rangle + (\mathbf{v}, \mathbf{D}^{\mathrm{T}}[\mathbf{A}]) = (\mathbf{v}, \mathbf{NA})_{\Gamma} \tag{C6}$$

which constitute two very useful partial integration formulas. In particular it may be derived that:

$$(\hat{\mathbf{L}}[\tilde{\mathbf{u}}], \mathbf{v}) = \langle \hat{\mathbf{H}}\mathbf{D}[\tilde{\mathbf{u}}], \mathbf{D}[\mathbf{v}] \rangle - (\mathbf{N}\hat{\mathbf{H}}\mathbf{D}[\tilde{\mathbf{u}}], \mathbf{v})_{\Gamma} \tag{C7}$$

and also ($\hat{\mathbf{L}}_a = \hat{\mathbf{L}}^*$ is the adjoint of $\hat{\mathbf{L}}$):

$$(\hat{\mathbf{L}}[\tilde{\mathbf{u}}], \mathbf{v}) = (\tilde{\mathbf{u}}, \hat{\mathbf{L}}_a[\mathbf{v}]) + (\tilde{\mathbf{u}}, \mathbf{N}\hat{\mathbf{H}}^{*\mathrm{T}}\mathbf{D}[\mathbf{v}])_{\Gamma} - (\mathbf{N}\hat{\mathbf{H}}\mathbf{D}[\tilde{\mathbf{u}}], \mathbf{v})_{\Gamma} \tag{C8}$$

$$\hat{\mathbf{L}}_a[\mathbf{v}] = -\mathbf{D}^{\mathrm{T}}[\hat{\mathbf{H}}^{*\mathrm{T}}\mathbf{D}[\mathbf{v}]]. \tag{C9}$$